Robust Control of Magnetic Bearing Systems by Means of Sliding Mode Control

K. NONAMI AND H. YAMAGUCHI

ABSTRACT The sliding mode control method from variable structure control theory is compared with conventional *PID* control method for the flexible rotor supported by magnetic bearings from the simulations and the experiments in two cases of the lift off and the rotations. It has been found that the sliding mode control is very effective and superior to *PID* control for magnetic bearing systems.

1. INTRODUCTION

It is common knowledge that magnetic bearing is open loop unstable system and supersensitive system for parameter deviations because the stiffness is negative by nature and the electromagnetic forces have a strong nonlinearity. Therefore magnetic bearing systems are generally controlled by *PID* type controller tuned based on trial and error without the mathematical model. However it takes much time and much labors to take the tuning of *PID* controller. So, a robust control is eagerly waited for in this field.

In this paper, the sliding mode control[1-2] , is a typical method of nonlinear adaptive control and robust control, is applied to magnetic bearing system. It has its roots in relay[4] and bang-bang control theory. Sliding mode control is a high speed switching feedback control, for example, the gains in each feedback path switch between two values according to some rules. This control law drive system's state trajectory to a user-chosen surface in the state space called the sliding surface for all subsequent time. The sliding surface is called switching surface in another name because if the state trajectory is above the surface a control path has one gain and a different gain if the trajectory drops below the surface. From this control, system is restricted to this surface and is stabilized. This method is a very robust for parameter change, modelling error and disturbance etc.

The sliding mode control method is compared with *PID* control method for the flexible rotor supported by magnetic bearings in two cases of the lift off and the rotation is both the simulation and experiments.

2. MODELING AND CONTROL STRATEGY

2.1 Basic Equation

This paper deals with a radial-type magnetic bearing system. Figure 1 shows four assembled electromagnetics. The whole system used for experiments is shown in Fig.2 where the flexible rotor shown is assumed rigid. We make the following assumptions:

(1) The attractive forces are proportional to the square of the coil current.

(2) Both electromagnetic bearings have the same characteristics.
(3) The induced voltages of electromagnets are ignored.
(4) The coil inductances are independent of frequency and gap length and are constant.
(5) This system is uncoupled between the x and y directions.
(6) Only small vibrations near equilibrium are considered.
(7) The rotor mass is concentrated at the bearing.

Under these conditions, we obtain the following equation for one electromagnet:

$$E=L\frac{dI}{dt}+RI \tag{1}$$

where E is the coil input voltage, L the coil inductance, R the coil registance, and I the coil current. The attractive force of an electromagnet can generally be given by

$$P=\frac{\mu_0 A N^2 I^2}{H^2} \tag{2}$$

where P is the attractive force, μ_0 the permeability, A the face area, N the number of winding turns, and H the gap length. From the standpoint of small vibration near equlibrium, $P,H,$ and I are given by

$$P=p_0+p, I=i_0+i, H=h_0+h \tag{3}$$

where p_0 is the stady-state attractive force, i_0 the steady-state current, h_0 the steady-state gap length, p the control attractive force, i the control current, and h the control gap length. Using the Taylor series expansion for small values of i and h and assuming $i \ll i_0$ and $p \ll p_0$, we can finally get the following attractive control force in linear term:

$$p=2p_o\left(\frac{i}{i_o}-\frac{h}{h_o}\right) \tag{4}$$

The four control attractive forces p_1,p_2,p_3 are $p_4$shown in Fig.1. The resultant forces of the horizontal control attractive force and the vertical control attractive force are, respectively,

$$\begin{aligned} m\ddot{x}&=p_1-p_3 \\ m\ddot{y}&=(p_s+p_2)-(p_o+p_4)-mg \end{aligned} \tag{5}$$

where m is the half-mass of the rigid rotor and g the acceleration of gravity. Assuming that control current to coils are $i_3=-i_1$ and $i_4=-i_2$, we have the following expressions considering Eq.(4):

$$\begin{aligned} m\ddot{x}&=-4p_o\left(\frac{i}{i_o}-\frac{x}{h_o}\right) \\ m\ddot{y}&=-2\left(\frac{p_s}{i_s}+\frac{p_o}{i_o}\right)i+2\left(\frac{p_s}{h_o}+\frac{p_o}{h_o}\right)y \end{aligned} \tag{6}$$

where the control gap length h is replaced by the displacement x and y from equilibrium; $mg+p_o$is replaced by the steady-state attractive force p_s and the steady-state current i_s.

The phase lead circuit is used to compensate for the time constant of electromagents in order to maintain control at higher frequencies. We can obtain the following equation concerning a phase lead circuit:

$$\frac{dv}{dt}=\frac{E_1}{CR_1}-\frac{R_1+R_2}{CR_1R_2}v \tag{7}$$

where the new parameter v is the phase lead voltage and R_1,R_2,C are parameters of the phase lead circuit. E_1 is the input voltage to the phase lead circuit. The integral values of displacements are used as control variables. The formulas are

$$\alpha = \int_0^t x dt,\ \beta = \int_0^t y dt \tag{8}$$

Replacing E with E_1- v in Eq.(1) since E=E_1-v. We get

$$\frac{di}{dt} = \frac{1}{L}(E_1\text{-}v)\frac{R}{L}i \tag{9}$$

Using Eqs.(5)~(9), we can write the state equation as next section.

2.2 State Equation The state equation for rigid rotor supported by magnetic bearings is written as follows[3]:

$$\dot{X} = A_H X + bu_x \tag{10}$$

$$\dot{Y} = A_V Y + bu_y \tag{11}$$

where A_H is the horizontal system matrix and A_V is the vertical system matrix. These are

$$A_H = \begin{bmatrix} 0 & 1 & 0 & 0 & 0 \\ \frac{4p_o}{mh_o} & 0 & 0 & -\frac{4p_o}{mi_o} & 0 \\ 1 & 0 & 0 & 0 & 0 \\ 0 & 0 & 0 & -\frac{R}{L} & -\frac{1}{L} \\ 0 & 0 & 0 & 0 & -\frac{R_1+R_2}{CR_1R_2} \end{bmatrix} \tag{12}$$

$$A_V = \begin{bmatrix} 0 & 1 & 0 & 0 & 0 \\ \frac{2}{m}(\frac{p_s}{h_o}+\frac{p_o}{h_o}) & 0 & 0 & -\frac{2}{m}(\frac{p_s}{i_s}+\frac{p_o}{i_o}) & 0 \\ 1 & 0 & 0 & 0 & 0 \\ 0 & 0 & 0 & -\frac{R}{L} & -\frac{1}{L} \\ 0 & 0 & 0 & 0 & -\frac{R_1+R_2}{CR_1R_2} \end{bmatrix} \tag{13}$$

The state vectors X and Y, the control vector b, and the control inputs u_x and u_y are given by

$$X = [\,x \ \ \dot{x} \ \ \alpha \ \ i_x \ \ v_x\,]^T \tag{14}$$

$$Y = [\,y \ \ \dot{y} \ \ \beta \ \ i_y \ \ v_y\,]^T \tag{15}$$

$$b = [\,0 \ \ 0 \ \ 0 \ \ \frac{1}{L} \ \ \frac{1}{CR_1}\,]^T \tag{16}$$

$$u_x = E_{1x}\ ,\ u_y = E_{1y} \tag{17}$$

where T means transpose. The output feedback control system of *PID* type is given by

$$u_x = -F_x X\ ,\ u_y = -F_y Y \tag{18}$$

where

$$\begin{aligned} F_x &= [f_{1x} \ \ f_{2x} \ \ f_{3x} \ \ f_{4x} \ \ f_{5x}] \\ F_y &= [f_{1y} \ \ f_{2y} \ \ f_{3y} \ \ f_{4y} \ \ f_{5y}] \end{aligned} \tag{19}$$

We assume the following expression as f_4 , $f_5 = 0$.

2.3 Sliding Mode Control The sliding mode control based on Variable Structure System (VSS) theory is the concept that the state of the system is restricted on the sliding surface by switching the control structure at both side on the super plane in the state space and the closed loop system is stabilized by the state restricted is sliding to the equilibrium on the switching surface. On the actual control system design in this paper, we assume the rotor system is rigid rotor as sections 2.1 and 2.2 and design the controller for the fifth order state equation. The constructed control system based on the sliding mode control theory has the feature of an on-off control in addition to conventional linear control. We tried many cases about switching widths of linear feedback gains. The best switching widths were almost 10 percent of each linear feedback gain.

The sliding mode control is a method which each feedback gain is switched at the rate of the specified percentage depending on each state of each state variable. Therefore, we have to design the switching surface on the state space at first. The switching surface is designed using various methods, for example, pole placement.

The switching surface is defined as follows:

$$\sigma = SX = [\, s_1 \;\; s_2 \;\; s_3 \;\; s_4 \;\; s_5 \,]X \tag{20}$$

The existence of a sliding mode implies the following state trajectory.

$$\sigma = 0 \tag{21}$$

$$\dot{\sigma} = 0 \tag{22}$$

The so-called equivalent control input is solved using Eq.(22) as follows:

$$\begin{aligned} \dot{\sigma} &= S\dot{X} \\ &= S(AX + Bu) \\ &= 0 \\ \therefore U_{eq} &= -(SB)^{-1}SAX \end{aligned} \tag{23}$$

The parameters of the switching surface are obtained by means of pole placement method.

Let us consider the existence of the sliding state. We assume the Lyapunov function as

$$V(\sigma) = 0.5\sigma^2 \tag{24}$$

Differentiating this function in respect of time, we have

$$\dot{V} = \sigma\dot{\sigma} \tag{25}$$

The function V is positive definite for all of state space. If dV/dt is negative definite, the system is secured from the existence and the reachability of sliding mode. Therefore the switching rule of the feedback gains should be selected such that Eq.(25) becomes negative definite any time and any states. Using Eqs.(20) and (25) and taking into account of $u = -KX$, $K = [\, k_1 \;\; k_2 \;\; k_3 \;\; k_4 \;\; k_5 \,]$,we get the final expression.

$$\begin{aligned} \dot{V} &= \sigma\dot{\sigma} \\ &= \sigma S\dot{X} \\ &= \sigma S(AX + Bu) \\ &= \sigma SAX - \sigma SBKX \\ &= SA\,\sigma X - SBK\,\sigma X < 0 \end{aligned} \tag{26}$$

Using Eq.(26), the switching feedback gains are

$$\begin{aligned} k_i = k_{i+} &> (SB)^{-1}(SA)_i \quad \sigma x_i > 0 \\ k_i = k_{i-} &< (SB)^{-1}(SA)_i \quad \sigma x_i < 0 \end{aligned} \qquad (i = 1, 2, 3, 4, 5) \tag{27}$$

3. SIMULATION

3.1 Simulations in the Case of Output Feedback The simulations of the

sliding mode control are compared with *PID* control on the same condition of experiments. From Eq.(23), we have $U_{eq} = -(SB)^{-1}SAX = -FX$. Therfore,the switching parameters are decided in the vertical direction as follows:

$$s_1=f_2, s_5=(f_5-\frac{a_4}{b_1})/(a_5-\frac{b_2}{b_1 a_4})$$
$$s_2=(f_4-s_4 a_3)/a_2,\ s_3=f_1-s_2 a_1,\ s_4=(1-s_5 b_2)/b_1$$

where

$$a_1=2/m(p_s/h_o+p_o/h_o), a_2=-2/m(p_s/i_s+p_o/i_o),$$
$$a_3=-R/L, a_4=-1/L,\ a_5=-(R_1+R_2)/CR_1R_2,$$
$$b_1=1/L,\ b_2=1/CR_1$$

The feedback gains used for experiments are $f_1=10400, f_2=250, f_3=11500$, so the switching parameters become $s_1=250$, $s_2=-957, s_3=11530, s_4=0.853, s_5=-0.0006$ in this case.

Figure 3 shows the impulse responses. The maximum displacement and the maximum control input in the case of the sliding mode control is smaller than the *PID* control. It is found that the sliding mode control is more effective for large displacements and the sliding mode is realized after 0.03 second from the switching function in Fig.3. Figure 4 shows the robustness concerning system parameter deviations. Figure 4 shows the responses before and after change when the 10 percent mass of the total rotor mass is added at levitation. The sliding mode control is superior to *PID* control for parameter deviations.

3.2 Simulations in the Case of State Feedback Exactly speaking, the sliding mode control with strong robustness should be realized by a full state feedback without observer on the point of view from theory. However it is difficult to carry out a full state feedback, therefore, the sate feedback using minimal order observer is applied to the sliding mode control in this section. We call this state feedback the linear control after this.

Figure 5 shows the step responses at lift off. The responses are improved and the settling time becomes short in the case of the sliding mode control. Also we can see switching control input in Fig.5. This typical phenomena are the reason why the sliding mode control can be applied to nonlinear control or adaptive control.

Even the steady-state current is changed to twice, the system is still stable in the case of the sliding mode control as shown in Fig.6. However the system becomes immediately unstable in *PID* control. Figure 7 shows the sensitivity characteristics in regard to unbalance forces as disturbance. From Fig.5, Fig.6 and Fig.7, the sliding mode control with state feedback is more excellent than the case with output feedback.

4. TEST RIG AND EXPERIMENTAL RESULTS

The block diagram of the schematic test rig is shown in Fig.2. The rotor mass is $3.6kg$ and the shaft length is about $1m$. The shaft diameter is $20mm$ and has two disks which each mass is $0.55kg$. The first and second bending critical speeds of this shaft system is about 55 Hz and 260 Hz. The displacements of the shaft are measured by the optical sensors close to magnetic bearings. These signals go to the digital signal processor (*DSP*) which is TMS320C25 with eight channels *A/D* and *D/A* converter. The rotor is supported in the radial direction by two active magnetic bearings as shown in Fig.6 and is connected with the flexible coupling in the axial direction. Four sliding mode controllers are independently designed each other, *AMB*#1 horizontal and vertical, *AMB*#2 horizontal and vertical. The switching rate of feedback gains is about 10 percent of linear gains in experiments and the switching time is 0.002 second. The sampling frequency is $4kHz$ in this experiments. The air gap between the electromagnet and the rotor disk is $1mm$ and the rotor contacts with the touch down bearings when the shaft

displacements exceed $0.7mm$.

In the experimental case of PID control, the feedback gains of the PID controller and parameters of the phase compensator are optimally tuned by manual with cut and try. It is not easy to compare the PID control with the sliding mode control on the same condition. The simulations of the PID control and the sliding mode control in chapter 3 were computed by using actual parameters used for experiments.

Figure 8 shows the impulse responses without rotation in the case of the same condition of Fig.3. The large amplitude is suppressed in the case of the sliding mode control.

Figure 9 indicates the experimental robust stability in the case when ten percent of the rotor mass is changed. Though the large vibration of the amplitude $20\mu m$ arises in the case of *PID* control as shown in Fig.9, the vibrations in the case of the sliding mode control is smaller than it. Figure 10 shows the unbalance responses at the location of *AMB*#1 and *AMB*#2. The violent vibration which means the contact with touch down bearings is recognized in the case of *PID* control because of unbalanced rotor at the location of *AMB*#1 in the horizontal direction, however the small vibrations in the case of the sliding mode control is observed compared with *PID* control. On the first bending critical speed about 55 Hz, the bending vibration was reduced to small vibration in the case of the sliding mode control. Namely, this means that sliding mode control has a stromg robustness. It was impossible to increase the rotating speed over $76Hz$ in *PID* control. By contrast, It was possible to increase the speed up to $160Hz$ (about $10000rpm$) within the maximum displacement $0.2mm$ because of small vibrations in the case of the sliding mode control. It is clear that the sliding mode control is very powerful for large vibration from simulations and experiments. In the case of linear control, the saturation in the power amplifier etc. is fatal result because the closed loop system becomes unstable. However, the saturation is not fatal in the case of the sliding mode control as shown in Fig.4 and Fig.10.

5. CONCLUSIONS The sliding mode control replacing with *PID* control in this paper is applied to active magnetic bearings using *DSP* control. From the simulations and the experiments, we have verified that the sliding mode control has a strong robustness for parameter deviations and an unbalance cancellation effect. Also it has become clear that the sliding mode control with robustness is superior to *PID* control for magnetic bearing control systems.

References

(1) Itokins, U., 1976. Control Systems of Variable Structure, John Wiley &Sons.

(2) Iwata, Y., Nakat,S., and Watanabe, A., 1991. "Sliding Mode Control of Flexible Arm." Transactions of the Japan Society of Mechanical Engineers, Ser.C, 57(534): 221-225.

(3) Nonami, K., 1988. "Vibration and Control of Flexible Rotor Supported by Magnetic Bearings." Proc. 1st Int. Sym. on Magnetic Bearings., Zurich, Switzerland, pp.177-186.

(4) Nonami, K., and Yamaguchi, H., 1991. "Active Vibration Control of Flexible Rotor for High Order Critical Speeds Using Magnetic Bearings." Proc. 2nd Int. Sym. on Magnetic Bearings., Tokyo, Japan, pp.155-160.

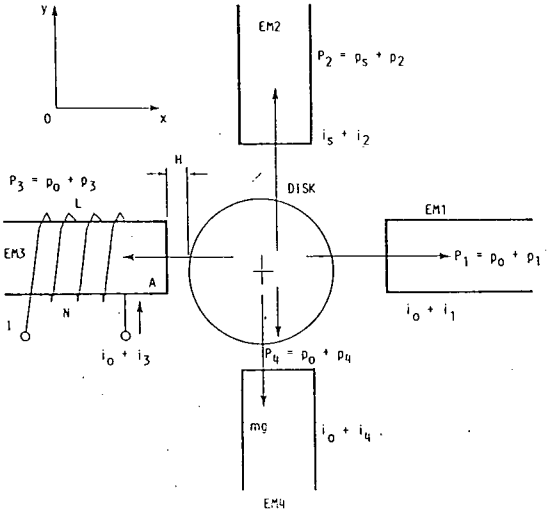

Fig.1 Four assembled electromagnets

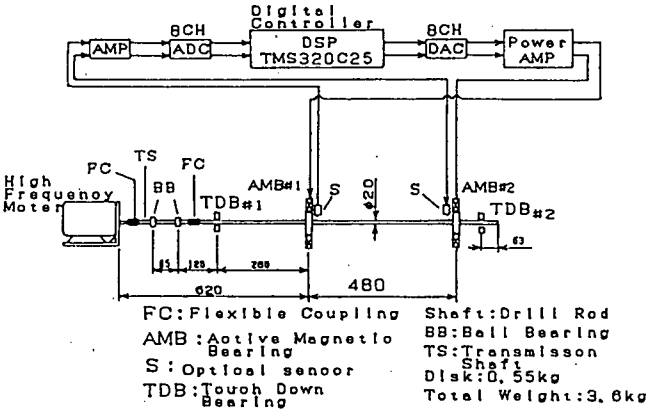

Fig.2 Schematic diagram of test rig

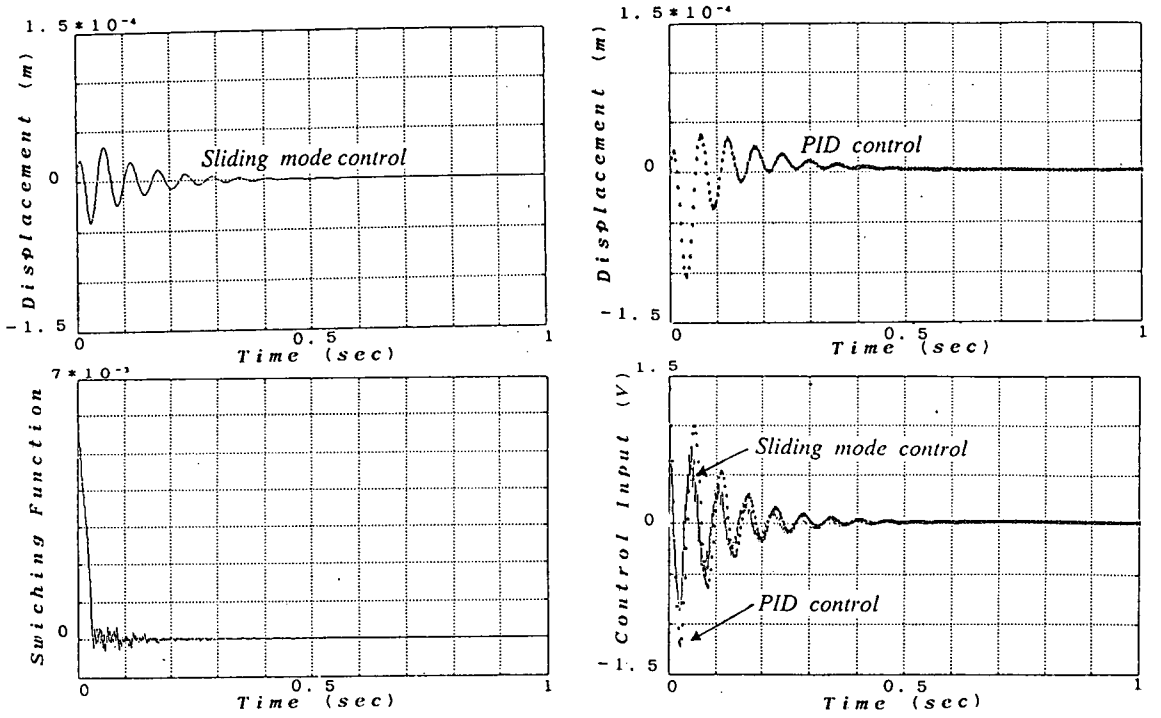

Fig.3 Comparison sliding mode control with PID control for impulse response

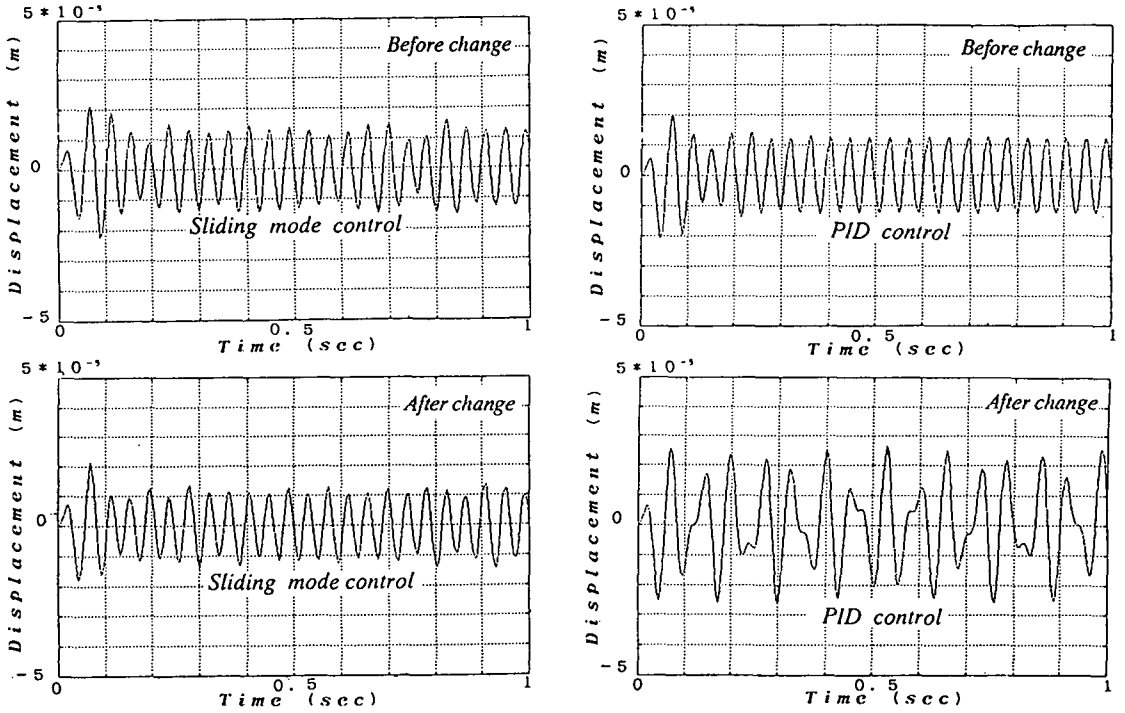

Fig.4 Comparison sliding mode control with PID control for parameter change

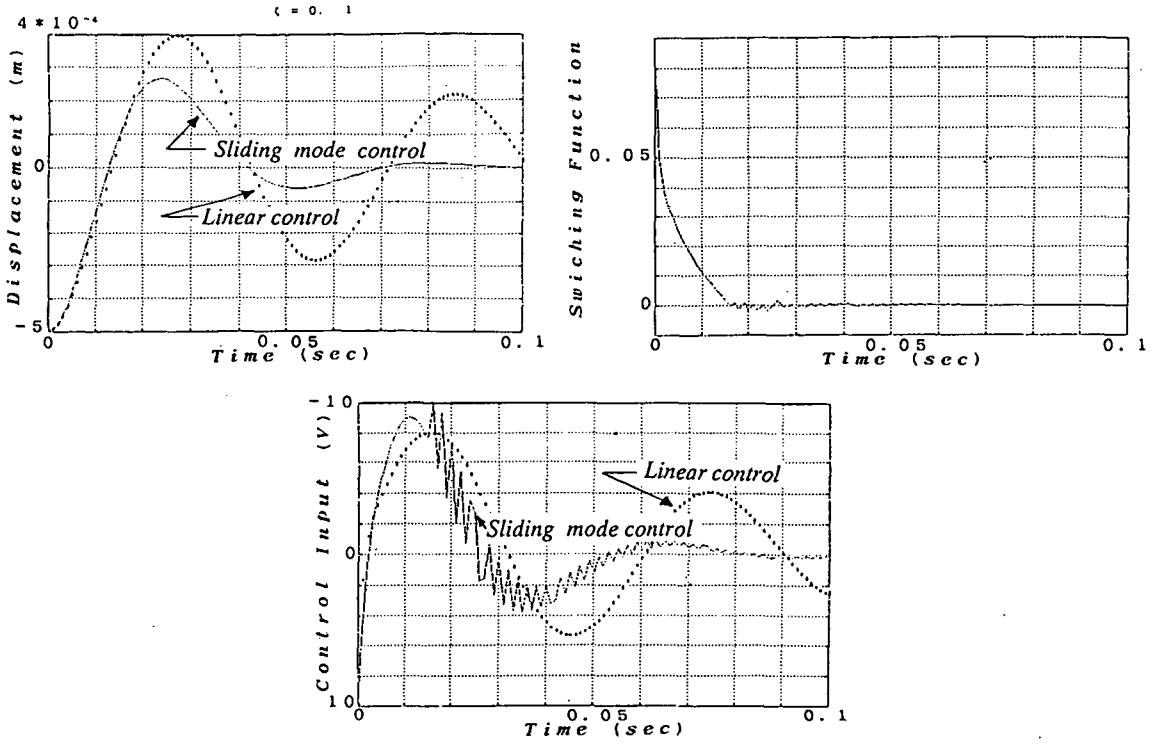

Fig.5 Comparison sliding mode control with linear control for step response

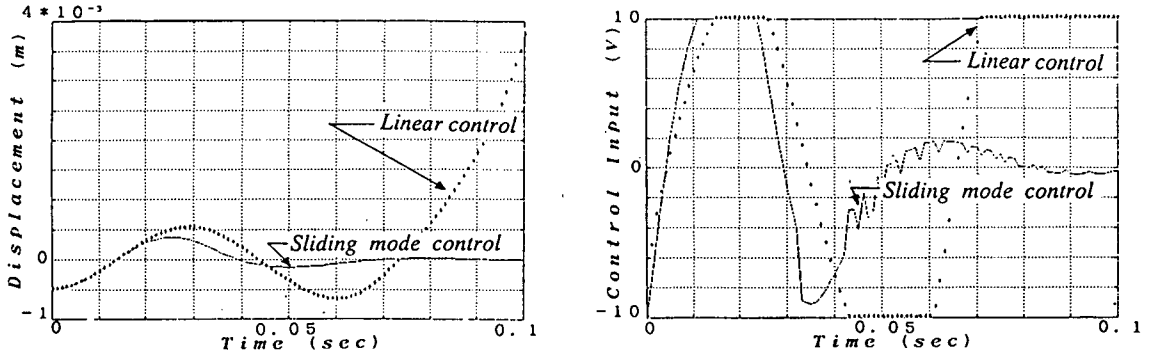

Fig.6 Comparison sliding mode control with linear control for parameter change

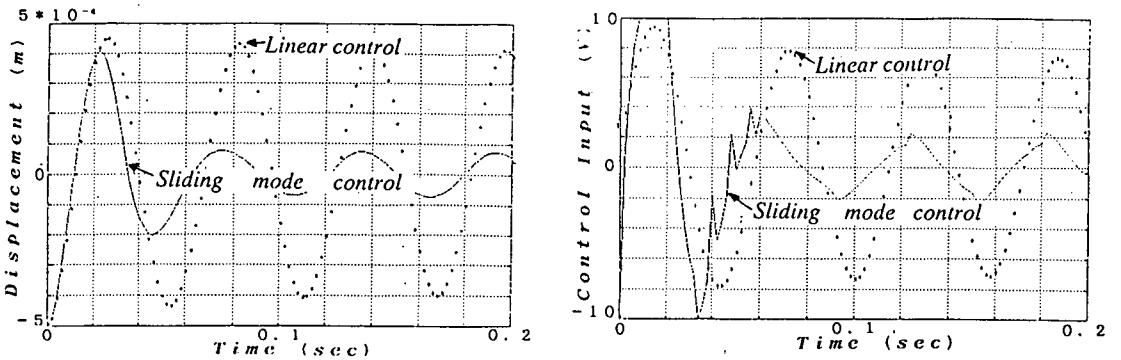

Fig.7 Comparison sliding mode control with linear control for sinsoidal disturbance

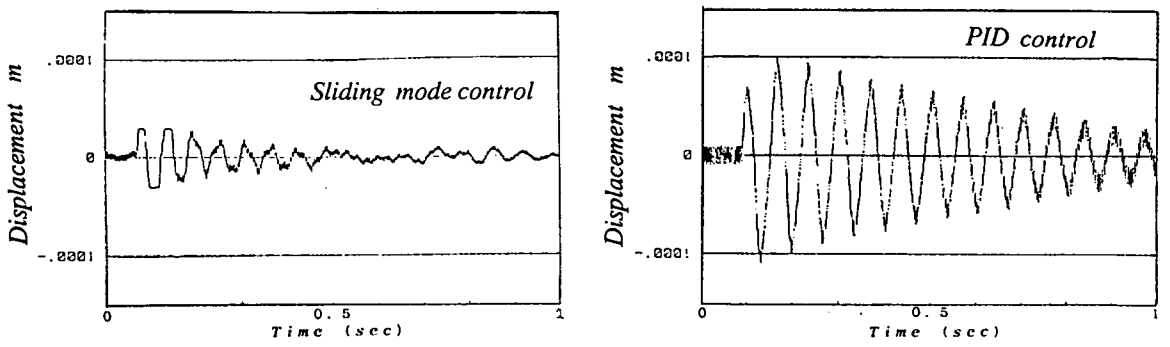

Fig.8 Comparison sliding mode control with PID control for impulse response (Experiments)

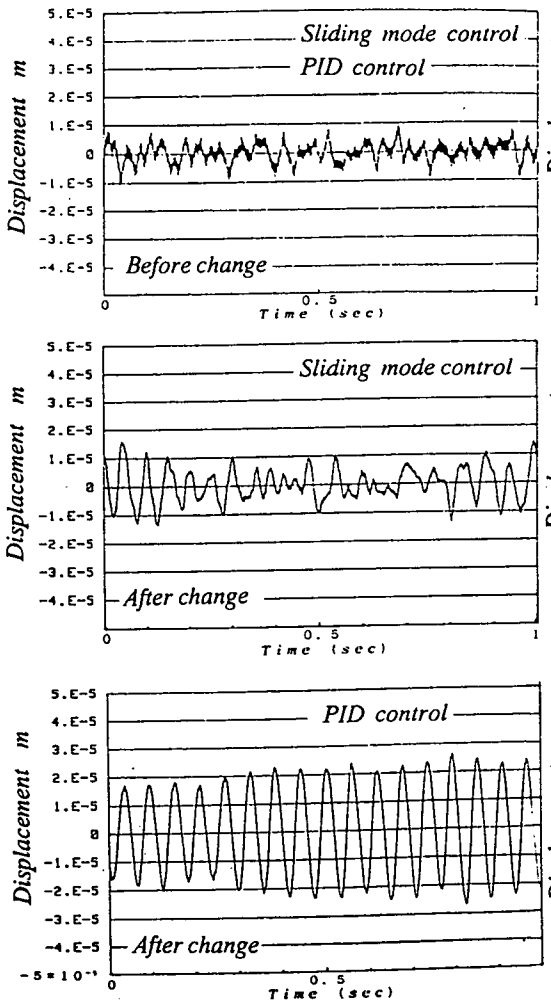

Fig.9 Comparison sliding mode control with PID control for parameter change (Experiments)

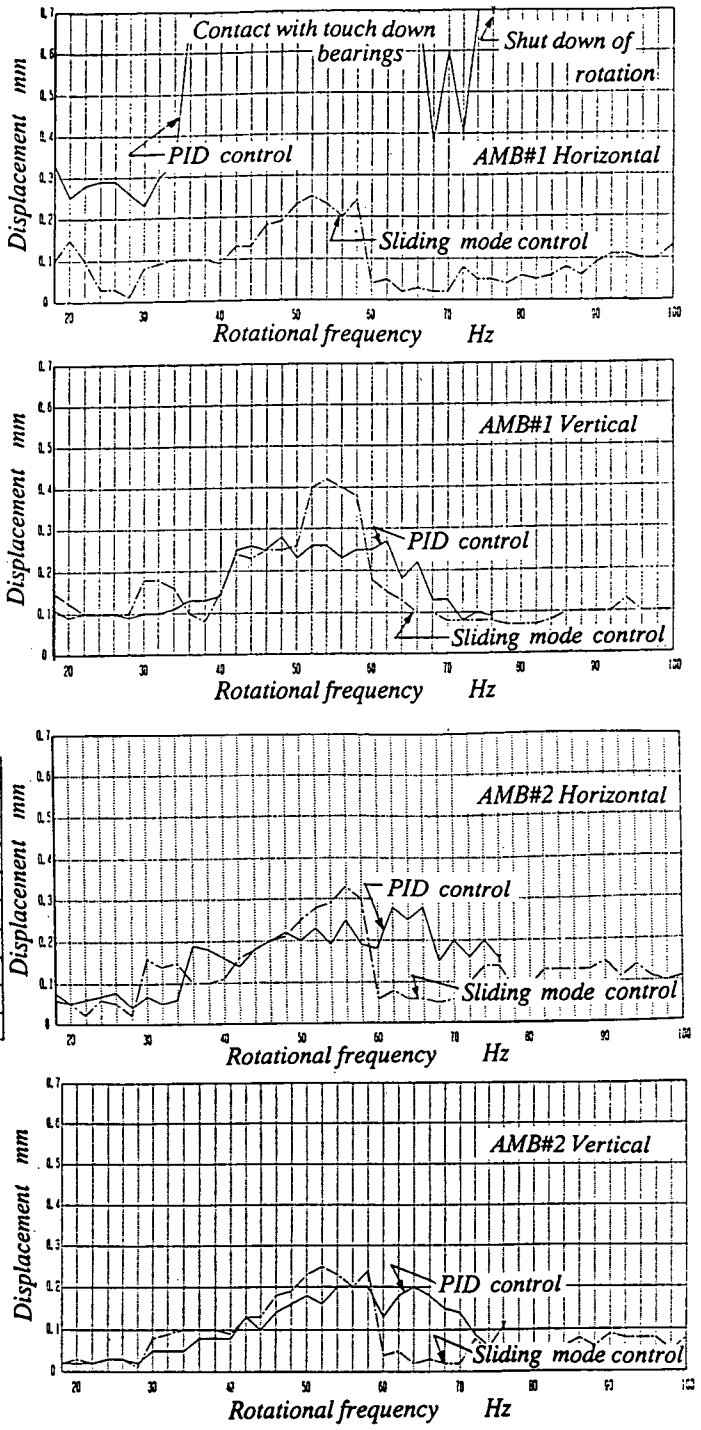

Fig.10 Comparison sliding mode control with PID control for steady-state unbalance response